




Quantitative thrombus characteristics on thin-slice computed tomography improve prediction of thrombus histopathology: results of the MR CLEAN Registry

Hajo Hund^{1,2,3,4} · Nikki Boodt^{2,3,5}  · Nerea Arrarte Terreros^{6,7} · Aladdin Taha^{3,4} · Henk A. Marquering^{6,7} · Adriaan C. G. M. van Es^{2,8} · Reinoud P. H. Bokkers⁹ · Geert J. Lycklama à Nijeholt¹ · Charles B.L.M. Majoie⁶ · Diederik W.J. Dippel³ · Hester F. Lingsma⁵ · Heleen M. M. van Beusekom⁴ · Aad van der Lugt² · on behalf of the MR CLEAN Registry Investigators

Received: 2 December 2021 / Revised: 14 March 2022 / Accepted: 21 March 2022 / Published online: 30 April 2022
© The Author(s) 2022

Abstract

Objectives Thrombus computed tomography (CT) characteristics might be used to assess histopathologic thrombus composition in patients treated with endovascular thrombectomy (EVT) for acute ischemic stroke (AIS). We aimed to assess the variability in thrombus composition that could be predicted with combined thrombus CT characteristics.

Methods Thrombi of patients enrolled in the MR CLEAN Registry between March 2014 and June 2016 were histologically analyzed with hematoxylin-eosin staining and quantified for percentages of red blood cells (RBCs) and fibrin/platelets. We estimated the association between general qualitative characteristics (hyperdense artery sign [HAS], occlusion location, clot burden score [CBS]) and thrombus composition with linear regression, and quantified RBC variability that could be explained with individual and combined characteristics with R^2 . For patients with available thin-slice (≤ 2.5 mm) imaging, we performed similar analyses for general and quantitative characteristics (HAS, occlusion location, CBS, [relative] thrombus density, thrombus length, perviousness, distance from ICA-terminus).

Results In 332 included patients, the presence of HAS ($a\beta$ 7.8 [95% CI 3.9–11.7]) and shift towards a more proximal occlusion location ($a\beta$ 3.9 [95% CI 0.6–7.1]) were independently associated with increased RBC and decreased fibrin/platelet content. With general characteristics, 12% of RBC variability could be explained; HAS was the strongest predictor. In 94 patients with available thin-slice imaging, 30% of RBC variability could be explained; thrombus density and thrombus length were the strongest predictors.

Conclusions Quantitative thrombus CT characteristics on thin-slice admission CT improve prediction of thrombus composition and might be used to further guide clinical decision-making in patients treated with EVT for AIS in the future.

Key Points

- With hyperdense artery sign and occlusion location, 12% of variability in thrombus RBC content can be explained.
- With hyperdense artery sign, occlusion location, and quantitative thrombus characteristics on thin-slice (≤ 2.5 mm) non-contrast CT and CTA, 30% of variability in thrombus RBC content can be explained.
- Absolute thrombus density and thrombus length were the strongest predictors for thrombus composition.

Keywords Ischemic stroke · Computed tomography · Thrombus · Thrombectomy · Histopathology

Abbreviations

CBS Clot burden score

CI	Confidence interval
IQR	Interquartile range
DT	Distance from ICA-terminus to thrombus in millimeters
HAS	Hyperdense artery sign
ICA	Internal carotid artery
R^2	Statistical measure: proportion of the variance for a dependent variable that is explained by variables in a regression model

Hajo Hund and Nikki Boodt contributed equally to this work.

✉ Nikki Boodt
n.boodt@erasmusmc.nl

Extended author information available on the last page of the article

RBC Red blood cell

Introduction

Despite the evident clinical benefit of endovascular thrombectomy (EVT) for acute ischemic stroke (AIS), about 20–30% of thrombi are resistant to the current retrieval approaches [1]. The histological composition of the occluding thrombus, i.e., the percentages of red blood cells (RBCs), fibrin, and platelets in the thrombus, has been associated with angiographic and clinical outcomes of EVT. Fibrin/platelet-rich (RBC-poor) thrombi have been shown to be stiffer and are associated with more retrieval attempts, longer procedure times, lower revascularization rates, and less favorable clinical outcomes than their RBC-rich counterparts [2–6]. It has been suggested that if accurate information on thrombus composition could be acquired prior to EVT, the interventionalist would be provided with a sense of what to expect during the procedure [7]. Moreover, information on the thrombus' histological composition may help guide treatment decisions, as scientific knowledge on thrombus-device interaction expands and thrombectomy devices specific for fibrin/platelet-rich thrombi are currently being developed [7–9].

Several thrombus characteristics can be assessed on non-contrast computed tomography (NCCT) and CT angiography (CTA), which are routinely conducted on hospital admission in patients with AIS. The presence of the hyperdense artery sign (HAS), based on visual identification of an artery with hyperdense attenuation, has been associated with RBC-rich (fibrin/platelet-poor) thrombi [5, 7, 10, 11]. The relationship of other general qualitative thrombus CT characteristics, such as occlusion location and clot burden score (CBS ranges from 0 to 10 and describes thrombus extent; a score of 10 is normal, and a score of 0 implies complete multisegment vessel occlusion [12]), with histological thrombus composition is not well-described.

As opposed to general qualitative thrombus CT characteristics, quantitative thrombus CT characteristics assessed on thin-slice (≤ 2.5 mm) CT [13–15] have the potential to provide a more accurate representation of thrombus subtype. Some studies have demonstrated the association of increased thrombus density (usually defined as the mean intraclot attenuation in Hounsfield units [HU] on NCCT) with increased RBC content of the thrombus [16–19], while others found no such association [3, 20–22]. Studies on the relationship between thrombus perviousness, which is a measure for thrombus permeability for contrast agent, and thrombus composition have reported heterogeneous results so far [21–24]. The relationship of thrombus length and measured distance from the internal carotid artery (ICA) terminus and thrombus composition has not been described previously.

Previous studies on the relationship of thrombus CT characteristics have been small in size and have mainly focused on one imaging characteristic at a time. Therefore, the value of a combination of thrombus CT characteristics to predict thrombus composition remains unknown. In this study, we aim to assess the relationship between various thrombus CT characteristics and thrombus composition, and to evaluate if thrombus composition can be predicted with individual and combined thrombus CT characteristics, in a large, multicenter registry of patients who underwent EVT for AIS.

Materials and methods

Setting and patients

We used data from the MR CLEAN (Multicenter Randomized Clinical Trial of Endovascular Treatment for Acute Ischemic Stroke in the Netherlands) Registry, which was a prospective observational study of all patients who underwent EVT for AIS in the Netherlands [25]. Enrollment started on 16 March 2014. All patients undergoing EVT (defined as at least entry into the angiography suite and receiving arterial puncture) for AIS, treated in one of the 16 centers performing EVT in the Netherlands, were registered. The central medical ethics committee of the Erasmus Medical Center Rotterdam, the Netherlands, approved the study protocol and granted permission to carry out the study as a registry (MEC-2014-235). Patients who met the following criteria were included in this study: age 18 years and older with a proximal intracranial vessel occlusion in the anterior circulation as demonstrated on CTA, and available thrombus for histological analysis. Data of patients treated until 15 June 2016 was collected and analyzed for this study.

Histological thrombus composition

Histological analyses were performed according to previously described methods [26]. Directly after EVT, retrieved thrombi were fixated in 4% buffered formaldehyde. Thrombi were embedded in paraffin with the largest cross-sectional area available for sectioning, typically along the length of the thrombus. Thrombi retrieved with multiple passes were collected and analyzed together. Two 5- μ m sections were acquired at representative depths, generally at 170 μ m and 230 μ m. Staessens and colleagues have shown that in large studies, one section per thrombus already provides accurate representation of thrombus composition [26]. Sections were stained with hematoxylin-eosin (H&E, HT110216, Sigma-Aldrich) and microscopical digital images were acquired with a slide scanner at 40 \times magnification (228 nm/pixel, 2.0 HT Nanozoomer, Hamamatsu Photonics). We quantitatively assessed RBC content and fibrin/platelet content, expressed

as percentage of total thrombus section area, with the use of Orbit Image Analysis software (version 3.15, Idorsia Pharmaceuticals Ltd).

Thrombus computed tomography characteristics

A central imaging core laboratory consisting of 21 observers (20 interventional neuroradiologists and 1 interventional neurologist, with at least 5–10 years of experience in diagnostic imaging and blinded for thrombus composition and all clinical information except for symptom side) assessed admission NCCT and CTA for general qualitative thrombus CT characteristics: presence of HAS, occlusion location, and CBS. Occlusion location (internal carotid artery [ICA], ICA-terminus, middle cerebral artery [proximal M1, distal M1, M2], anterior cerebral artery [A1, A2]) was based on the occluded segment on CTA.

In addition, quantitative thrombus CT characteristics were assessed in a subset of patients with available thin-slice (≤ 2.5 mm) NCCT and CTA imaging, acquired within 30 min from each other (available for 94 of 332 patients). Two neuroradiologists (7–8 years of experience in diagnostic imaging and blinded for thrombus composition) assessed absolute thrombus density, relative thrombus density, thrombus length, perviousness, and distance from the ICA-terminus to the thrombus (DT), according to previously described methods [13–15]. NCCT and CTA images were co-registered using rigid registration with Elastix [27]. Three spherical markers with a 1-mm radius were placed in the proximal, middle, and distal parts of the thrombus, on co-registered NCCT and CTA. Subsequently, three markers were symmetrically placed in the contralateral artery. Absolute thrombus density was defined as the mean density (in HU) of the three NCCT markers. Relative thrombus density was calculated by dividing the mean density of the thrombus by the mean density of the contralateral artery. Thrombus perviousness was estimated by subtracting the thrombus' mean density on NCCT from its mean density on CTA. Additionally, one marker was placed at the proximal thrombus border and one marker at the distal thrombus border. Thrombus length was defined as the largest extension of contrast filling defect in the occluded vessel on CTA (in mm). Whenever the proximal or distal border of the thrombus could not be depicted on CTA, thrombus length was based on the hyperdense artery sign on the co-registered NCCT [28]. Lastly, DT represents the distance from the ICA-terminus to the beginning of the thrombus (in mm) and was manually measured on CTA using axial, coronal, and/or sagittal views [29]. For thrombi located in the supra-clinoid segment of the ICA but not extending into the ICA-terminus, DT was set to zero.

Statistical analysis

For illustration, patient and baseline characteristics of the study population were tabulated according to tertiles of RBC

content. The association of HAS, occlusion location, and CBS with thrombus composition (RBC content and fibrin/platelet content, expressed as percentage of the thrombus) was estimated with univariable and multivariable linear regression models and presented as (adjusted) coefficients (α/β) with 95% confidence intervals (CI). We performed two multivariable analyses. In the first multivariable model, we adjusted for the clinical variables age, sex, time from stroke onset to CT, and administration of intravenous alteplase. In the second model, we adjusted for thrombus CT characteristics. For the regression analyses, we treated occlusion location as a continuous variable, increasing from proximal to distal (ICA; ICA-T; proximal M1; distal M1; M2/A2). Additionally, in the subgroup with available thin-slice imaging, we assessed the association of HAS, occlusion location, CBS, absolute thrombus density, relative thrombus density, thrombus length, perviousness, and DT with thrombus composition, in a similar manner.

We estimated the variability in thrombus composition (RBC content and fibrin/platelet content) that was explained with thrombus CT characteristics with R^2 . R^2 expresses the proportion of variance of a dependent variable that is explained by variables in a regression model. We reported R^2 for increasingly extensive models, in which one CT characteristic at a time was added to the model. The order in which CT characteristics were added was based on our perceived clinical availability and easiness in assessment, starting with the characteristic that was easiest to acquire (HAS). Furthermore, we assessed the value of each individual thrombus CT characteristic, by assessing the uniquely added R^2 to the full model (partial R^2) for each thrombus CT characteristic. For the analyses, missing data were imputed using multiple imputation. Variables that were imputed are listed in the Data Appendix (Table 4 in the Data Appendix). STATA/SE 16.0 (StataCorp LLC) was used for all statistical analyses.

Results

During the inclusion period, 1627 patients were registered. After excluding patients based on the prespecified criteria ($n = 1295$), 332 patients qualified for the assessment of general qualitative thrombus CT characteristics. Of 332 patients, 94 patients had an available thin-slice imaging for assessment of quantitative thrombus CT characteristics (Appendix Figure 4).

Of the 332 included patients, median age was 70 (interquartile range [IQR] 60–79) years, 177 (53%) were men, and median National Institutes of Health Stroke Scale on admission was 17 (IQR 13–20). The most common occlusion location was the proximal M1 ($n = 99$, 31%). HAS was present in 189 (60%) patients and median CBS was 6 (IQR 4–7). The majority of patients ($n = 251$, 76%) had received intravenous alteplase before EVT (Table 1). Median RBC content was 27% (IQR 16–42) and median fibrin/platelet content was 67% (IQR 53–78)

Table 1 Baseline, imaging, and workflow characteristics of patients in the current study, shown by tertiles of RBC content

	≤19.8% RBCs (n = 111)	19.9–36.7% RBCs (n = 111)	> 36.8% RBCs (n = 110)	Total (n = 332)
Age, year, median (IQR)	71 (58–80)	70 (63–79)	70 (59–76)	70 (60–79)
Men, n (%)	50 (45)	61 (55)	66 (60)	177 (53)
NIHSS, median (IQR)	17 (11–20)	18 (13–20)	17 (14–21)	17 (13–20)
Systolic blood pressure, mmHg, mean (SD)	147 (23)	149 (24)	151 (26)	149 (24)
Intravenous alteplase treatment, n (%)	85 (77)	85 (77)	81 (74)	251 (76)
Hyperdense artery sign, n (%)	48 (46)	63 (60)	78 (73)	189 (60)
Clot burden score, median (IQR)	6 (4–8)	6 (4–7)	5 (2–6)	6 (4–7)
<i>Medical history</i>				
Diabetes mellitus, n (%)	20 (18)	23 (21)	14 (13)	57 (17)
Hypertension, n (%)	58 (54)	61 (56)	59 (54)	178 (55)
Atrial fibrillation, n (%)	34 (31)	31 (28)	27 (25)	92 (28)
Ischemic stroke, n (%)	23 (21)	26 (24)	17 (16)	66 (20)
Peripheral artery disease, n (%)	17 (16)	9 (8)	17 (16)	43 (13)
Current smoking, n (%)	35 (32)	26 (23)	26 (24)	74 (22)
<i>Collateral grade</i>				
0, n (%)	3 (3)	10 (10)	14 (14)	27 (9)
1, n (%)	40 (39)	36 (36)	33 (32)	109 (36)
2, n (%)	35 (34)	42 (42)	36 (35)	113 (37)
3, n (%)	26 (25)	13 (13)	19 (19)	38 (19)
<i>Occlusion location subgroups</i>				
Intracranial ICA, n (%)	2 (2)	4 (4)	6 (6)	12 (4)
ICA-terminus, n (%)	19 (18)	27 (26)	44 (41)	90 (28)
Proximal M1, n (%)	34 (32)	29 (28)	36 (34)	99 (31)
Distal M1, n (%)	39 (36)	34 (33)	18 (17)	91 (29)
M2, n (%)	13 (12)	9 (9)	3 (3)	25 (8)
A1/A2, n (%)	1 (1)	0 (0)	0 (0)	1 (0)
<i>Workflow</i>				
Time from stroke onset to CT, min, median (IQR)	72 (60–110)	65 (50–113)	69 (53–115)	69 (53–114)
Time from stroke onset to groin puncture, min, median (IQR)	200 (155–260)	205 (155–266)	209 (166–260)	205 (160–260)

IQR indicates interquartile range, NIHSS National Institutes of Health Stroke Scale

SD standard deviation, ICA internal carotid artery, M1 and M2 middle cerebral artery, A1 and A2 anterior cerebral artery, CT computed tomography

(Appendix Figure 5). In the 94 patients with thin-slice imaging, median absolute thrombus density was 54.3 (IQR 46.4–59.6) HU, median relative thrombus density was 1.4 (IQR 1.2–1.6), median thrombus length was 15 (IQR 10–19) mm, median thrombus perviousness was 4.3 (IQR – 0.7 to 10.9) HU, and median DT was 5 (IQR 0–11) mm.

Association of thrombus CT characteristics with thrombus composition

Thrombus CT characteristics were associated with thrombus composition (Figs. 1 and 2). In all patients (n = 332), the presence of HAS (β 9.8 [95% CI 5.8 to 13.7]), shift towards a more proximal occlusion location (β – 5.5 [95% CI – 7.5 to – 3.5]), and lower CBS (β – .9 [95% CI – 2.7 to – 1.1]) were associated with increased RBC content (Table 2) and with

decreased fibrin/platelet content (Appendix Table 5) in the univariable analyses. Adjustment for clinical characteristics did not change these associations. When we adjusted for thrombus CT characteristics, HAS and occlusion location were independently associated with RBC content and fibrin/platelet content, while CBS was not.

In the subgroup with available thin-slice imaging (n = 94), absolute thrombus density (β 0.9 [95% CI 0.5 to 1.3]), thrombus length (β 0.9 [95% CI 0.5 to 1.4]), decreased thrombus perviousness (β – 0.4 [95% CI – 0.6 to – 0.1]), and decreased DT (β – 0.6 [95% CI – 1.1 to – 0.0]) were associated with increased RBC content (Table 3) and with decreased fibrin/platelet content (Appendix Table 6) in the univariable analyses. These associations remained unchanged when we adjusted for the clinical variables. When we adjusted for thrombus CT characteristics, absolute thrombus density and thrombus

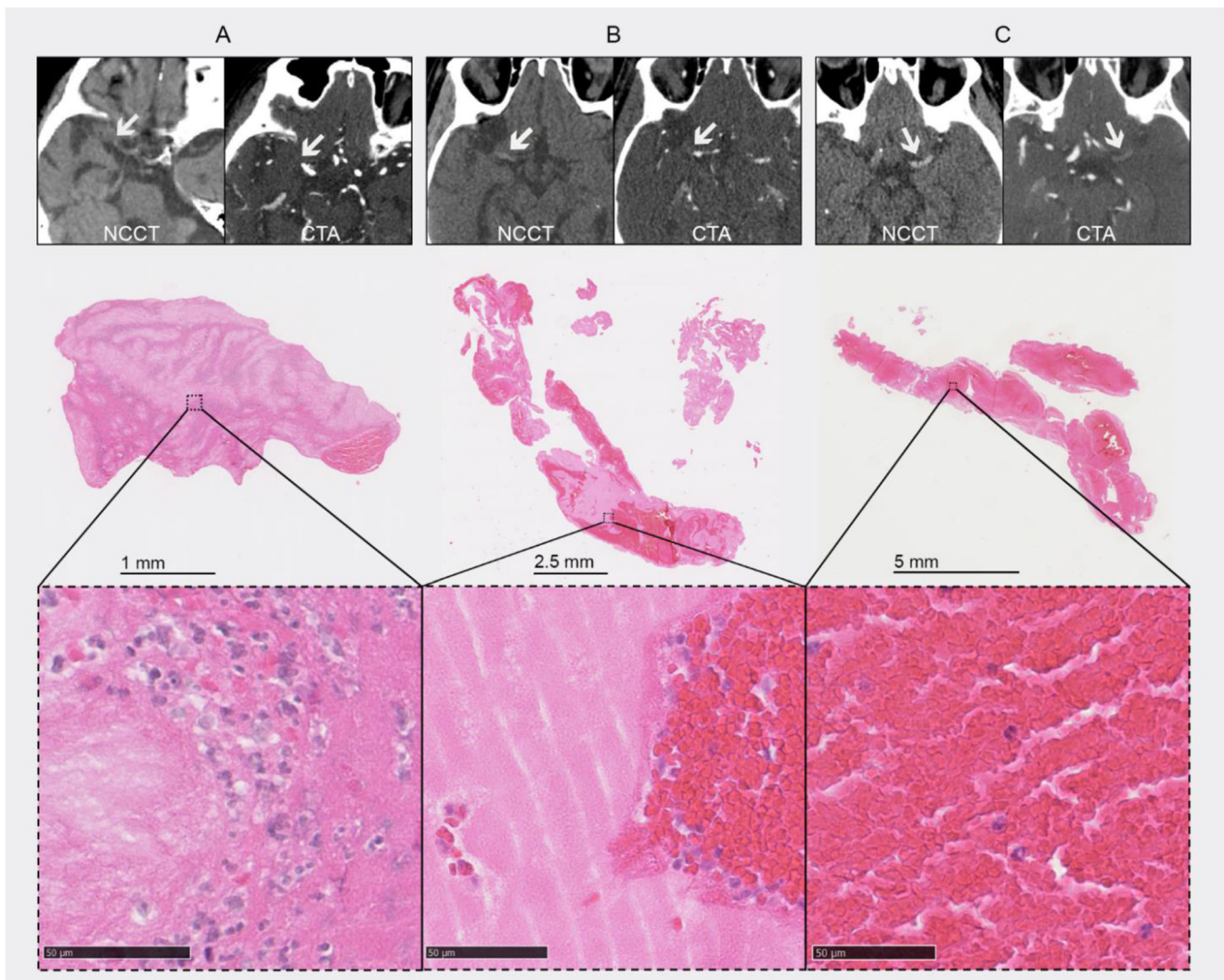


Fig. 1 Thrombi on computed tomography and the corresponding histological images, shown according to increasing red blood cell (RBC) content. From left to right (mean absolute thrombus density, RBC content): 32.4 HU, 4.3% (A); 54.0 HU, 25.6% (B); and 61.5 HU, 75.4% (C)

length were independently associated with thrombus composition, while all other characteristics were not (Table 3).

Explained variability in thrombus composition

Of the general thrombus CT characteristics (HAS, occlusion location and CBS, $n = 332$), HAS was the strongest predictor for RBC content, followed by occlusion location (Fig. 3a). A model including HAS and occlusion location explained 12% of the variability in RBC content of the thrombus (Fig. 3b). Adding CBS did not improve the performance of this model.

Of all thrombus CT characteristics (HAS, occlusion location, CBS, [relative] thrombus density, thrombus length, perviousness, and DT, in the subset of patients with thin-slice imaging, $n = 94$), absolute thrombus density and thrombus length were the strongest predictors for RBC content (Fig. 3c). The most extensive model, including all thrombus CT

characteristics, explained 30% of the variability in RBC content of the thrombus (Fig. 3d).

Discussion

In this study, we have shown that thrombus CT characteristics are associated with the histological composition of the occluding thrombus in patients treated with EVT for AIS. Additionally, we have demonstrated that about 30% of the variability in thrombus composition can be explained with a combination of thrombus CT characteristics derived from admission thin-slice NCCT and CTA.

In line with previous literature, we found that the presence of HAS was associated with increased RBC content and decreased fibrin/platelet content of the thrombus [5, 7]. We also observed a clear relationship between increased absolute thrombus density and increased RBC content and decreased

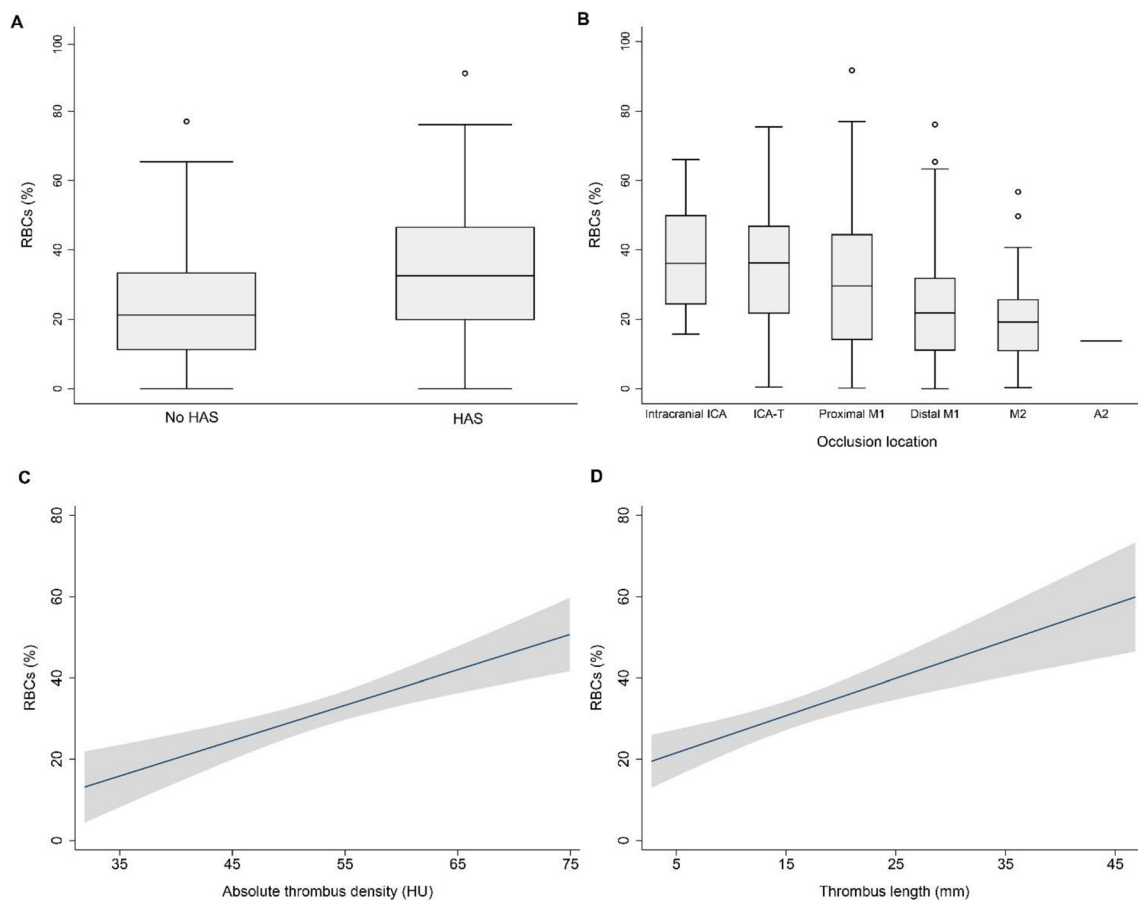


Fig. 2 Boxplots of the relationship of hyperdense artery sign (HAS) and occlusion location with red blood cell (RBC) content (**A** and **B**, $n = 332$) and fitted curves with 95% confidence intervals for the relationship of absolute thrombus density and thrombus length with RBC content (**C** and **D**, $n = 94$)

fibrin/platelet content, which is in line with most studies on this topic [16–19], but not with some others [3, 20–22]. Noteworthy, the majority of studies that found a relationship between thrombus density and thrombus composition used imaging with 5-mm slice thickness and one region of interest for the assessment of thrombus density, while the value of thin-slice imaging and multiple regions of interest has been shown [13]. Interestingly, we did not observe a relationship between relative thrombus density and thrombus composition, which is in contrast to earlier findings [17, 22]. Relative thrombus density is calculated from regions of interest in the

thrombus as well as in the contralateral artery, and has been shown to have higher interobserver variability than absolute thrombus density [13], which could be an explanation for our conflicting findings. We observed a weak association between decreased thrombus perviousness and increased RBC content, which is in line with previous contrasting findings regarding the relationship between thrombus perviousness and thrombus histology [21–24]. Increased thrombus length on CT was associated with increased RBC content and decreased fibrin/platelet content. To our knowledge, this relationship has not been described in previous literature.

Table 2 Univariable and multivariable linear regression analyses for the relationship between thrombus CT characteristics and thrombus RBC content, in all included patients ($n = 332$)

	Unadjusted	Adjusted for clinical characteristics*	Adjusted for thrombus CT characteristics†
Hyperdense artery sign	9.8 (5.8 to 13.7)	9.8 (5.8 to 13.7)	7.8 (3.9 to 11.7)
Occlusion location	− 5.5 (− 7.5 to − 3.5)	− 5.5 (− 7.6 to − 3.5)	− 3.9 (− 7.1 to − 0.6)
Clot burden score	− 1.9 (− 2.7 to − 1.1)	− 1.9 (− 2.7 to − 1.1)	− 0.4 (− 1.7 to 0.9)

Regression coefficients are shown with 95% confidence intervals. All analyses were done with RBC content as a continuous variable, expressed as percentage of the thrombus

*Age, sex, time from stroke onset to CT, and administration of IV alteplase

†Hyperdense artery sign, occlusion location, and clot burden score

Table 3 Univariable and multivariable linear regression analyses for the relationship between thrombus CT characteristics and thrombus RBC content, in patients with available thin-slice CT imaging (*n* = 94)

	Unadjusted	Adjusted for clinical characteristics*	Adjusted for thrombus CT characteristics†
Hyperdense artery sign	5.5 (− 2.4 to 13.3)	5.7 (− 2.1 to 13.5)	− 3.7 (− 11.7 to 4.2)
Occlusion location	− 4.4 (− 8.4 to − 0.4)	− 4.0 (− 8.1 to 0.1)	− 4.1 (− 13.5 to 5.4)
Clot burden score	− 1.7 (− 3.3 to − 0.1)	− 1.4 (− 3.0 to 0.2)	1.0 (− 2.2 to 4.1)
Absolute thrombus density (HU)	0.9 (0.5 to 1.3)	0.8 (0.5 to 1.2)	0.8 (0.3 to 1.4)
Thrombus length (mm)	0.9 (0.5 to 1.3)	0.8 (0.4 to 1.3)	0.8 (0.2 to 1.4)
Relative thrombus density (HU)	13.1 (− 0.8 to 27.1)	14.2 (0.4 to 28.0)	− 10.4 (− 26.8 to 6.1)
Perviousness (HU)	− 0.4 (− 0.6 to − 0.1)	− 0.4 (− 0.6 to − 0.1)	− 0.2 (− 0.4 to 0.0)
DT (mm)	− 0.6 (− 1.1 to − 0.0)	− 0.5 (− 1.0 to 0.1)	0.6 (− 0.3 to 1.5)

Regression coefficients are shown with 95% confidence intervals. All analyses were done with RBC content as a continuous variable, expressed as percentage of the thrombus. HU indicates Hounsfield units and DT, distance from internal carotid artery terminus to thrombus

*Age, sex, time from stroke onset to CT, and administration of IV alteplase

†Hyperdense artery sign, occlusion location, clot burden score, absolute thrombus density, thrombus length, relative thrombus density, perviousness and distance from internal carotid artery terminus to the thrombus

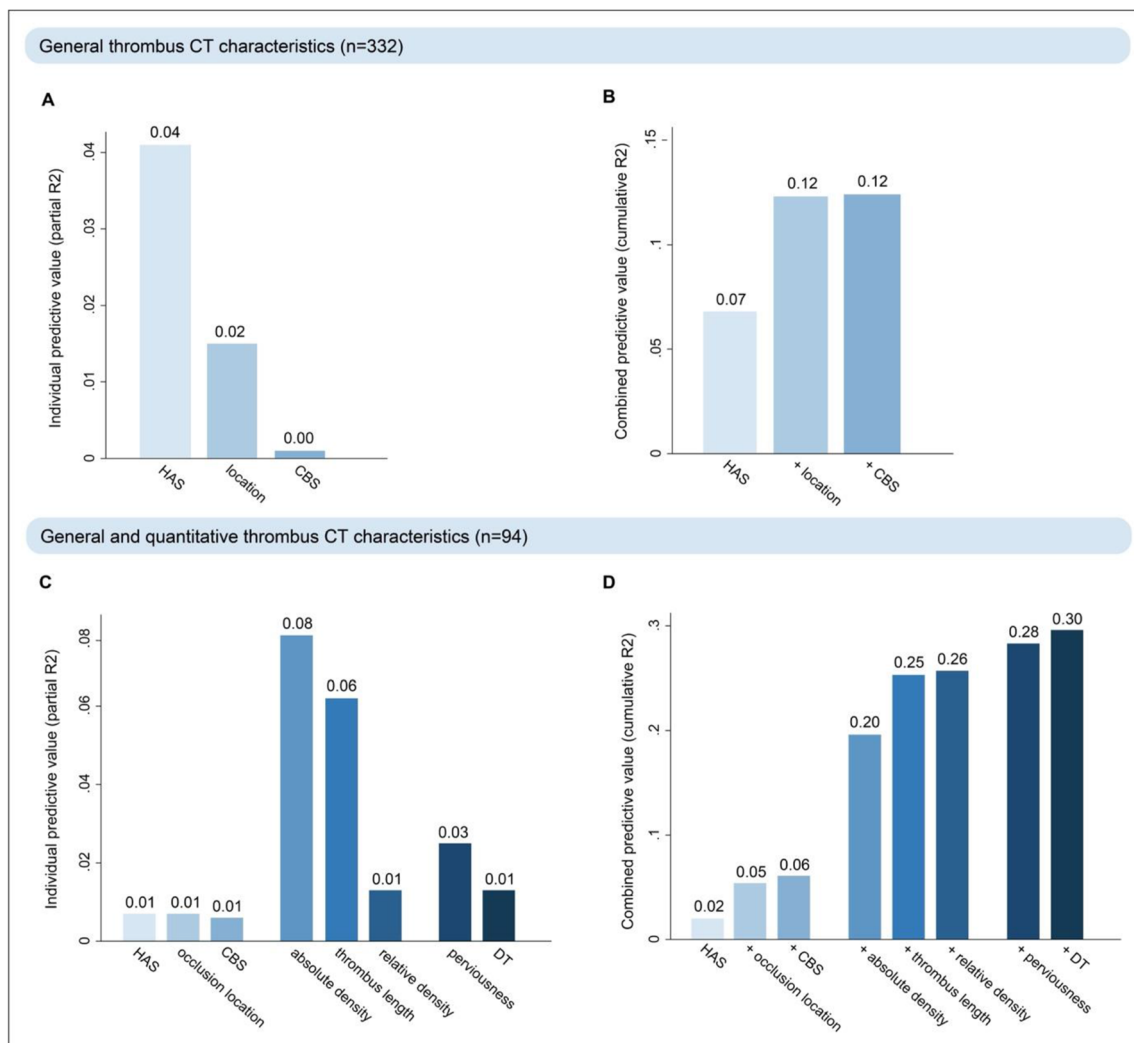


Fig. 3 Explained variability in thrombus red blood cell (RBC) content by thrombus CT characteristics is shown. Of the general qualitative characteristics (hyperdense artery sign [HAS], occlusion location and clot burden score [CBS]), HAS was the strongest predictor (A) and 12% of RBC variability could be explained with these characteristics

combined (B). In patients with available thin-slice imaging, thrombus density and thrombus length were the strongest predictors (C) and 30% of RBC variability could be explained with all thrombus CT characteristics combined (D)

However, in line with our findings, a more proximal occlusion location has previously been associated with increased RBC content [30]. Since smaller thrombi are more likely to travel further into the intracranial circulation [31], this relationship might be explained due to collinearity between thrombus length and location.

The value of combined thrombus CT characteristics for the prediction of histological thrombus composition is not well-described. In this study, we have shown that quantitative thrombus CT characteristics substantially improved prediction of thrombus composition: With a combination of general and quantitative thrombus CT characteristics, 30% of the variability in thrombus composition could be explained, as opposed to 12% when only general thrombus CT characteristics were available. Future studies should aim to confirm these findings.

Thrombus CT characteristics as a potential guide for EVT approach

Recent *in vitro* studies have shown that with stent retrievers, better results are achieved for soft, RBC-rich thrombi than for stiffer, fibrin/platelet-rich thrombi [3, 7]. Therefore, it has been suggested that selection of first-line device (i.e., aspiration versus stent retriever thrombectomy) might be based on thrombus composition in the future. Moreover, research on next-generation EVT devices currently focuses on specific designs for fibrin-rich thrombi. In the current study, we have shown that a substantial part of thrombus composition can be explained with thrombus CT characteristics. Future studies could focus on whether certain thrombectomy techniques or devices tailored to thrombus CT characteristics, such as density and length, result in better outcomes, to eventually reach complete reperfusion in all patients.

Limitations

This study has limitations. First, a large proportion of patients who underwent EVT was not included in the study, because the thrombus was not kept for histological processing at the participating center or no thrombus was retrieved during the intervention. Unfortunately, we did not keep track of in which cases a retrieved thrombus was not sent in for histology, which is a consequence of a multicenter registry of daily clinical practice. Furthermore, studies have shown that RBC-rich thrombi, or parts of the thrombus that are RBC-rich, are more likely to be successfully retrieved with EVT. Therefore, fibrin/platelet-rich thrombi might have been underrepresented in our study. Moreover, for the quantification of histological thrombus components, it is assumed that thrombus composition is homogeneous throughout the thrombus, while in reality, thrombi are highly heterogeneous. However, Staessens and colleagues have shown that in large studies, one section per thrombus already provides accurate representation of total

thrombus composition. Lastly, fibrin and platelets cannot be easily distinguished from each other on H&E staining. While most previous studies on histological thrombus composition quantified components in the same manner as we did, future studies should assess fibrin and platelets separately.

Conclusions

Quantitative thrombus CT characteristics derived from thin-slice (≤ 2.5 mm) admission NCCT and CTA imaging improve prediction of thrombus composition and might be used to guide clinical decision-making in patients treated with EVT for AIS in the future.

Appendix

MR CLEAN Registry Investigators – group authors

Executive committee

Diederik W.J. Dippel¹; Aad van der Lugt²; Charles B.L.M. Majoie³; Yvo B.W.E.M. Roos⁴; Robert J. van Oostenbrugge⁵; Wim H. van Zwam⁶; Jelis Boiten¹⁴; Jan Albert Vos⁸

Study coordinators

Ivo G.H. Jansen³; Maxim J.H.L. Mulder^{1,2}; Robert-Jan B. Goldhoorn^{5,6}; Kars C.J. Compagne²; Manon Kappelhof³; Josje Brouwer⁴; Sanne J. den Hartog^{1,2,40}; Wouter H. Hinsenfeld^{5,6};

Local principal investigators

Diederik W.J. Dippel¹; Bob Roozenbeek¹; Aad van der Lugt²; Adriaan C.G.M. van Es²; Charles B.L.M. Majoie³; Yvo B.W.E.M. Roos⁴; Bart J. Emmer³; Jonathan M. Coutinho⁴; Wouter J. Schonewille⁷; Jan Albert Vos⁸; Marieke J.H. Wermer⁹; Marianne A.A. van Walderveen¹⁰; Julie Staals⁵; Robert J. van Oostenbrugge⁵; Wim H. van Zwam⁶; Jeannette Hofmeijer¹¹; Jasper M. Martens¹²; Geert J. Lycklama à Nijeholt¹³; Jelis Boiten¹⁴; Sebastiaan F. de Bruijn¹⁵; Lukas C. van Dijk¹⁶; H. Bart van der Worp¹⁷; Rob H. Lo¹⁸; Ewoud J. van Dijk¹⁹; Hieronymus D. Boogaarts²⁰; J. de Vries²²; Paul L.M. de Kort²¹; Julia van Tuijl²¹; Jo P. Peluso²⁶; Puck Fransen²²; Jan S.P. van den Berg²²; Boudewijn A.A.M. van Hasselt²³; Leo A.M. Aerden²⁴; René J. Dallinga²⁵; Maarten Uyttenboogaart²⁸; Omid Eschgi²⁹; Reinoud P.H. Bokkers²⁹; Tobien H.C.M.L. Schreuder³⁰; Roel J.J. Heijboer³¹; Koos Keizer³²; Lonneke S.F. Yo³³; Heleen M. den Hertog²²; Tomas Bulut³⁵; Paul J.A.M. Brouwers³⁴

Imaging assessment committee

Charles B.L.M. Majoie³(chair);Wim H. van Zwam⁶;Aad van der Lugt²;Geert J. Lycklama à Nijeholt¹³;Marianne A.A. van Walderveen¹⁰;Marieke E.S. Sprengers³;Sjoerd F.M. Jenniskens²⁷;René van den Berg³;Albert J. Yoo³⁸;Ludo F.M. Beenen³;Alida A. Postma⁶;Stefan D. Roosendaal³;Bas F.W. van der Kallen¹³;Ido R. van den Wijngaard¹³;Adriaan C.G.M. van Es²;Bart J. Emmer³;Jasper M. Martens¹²;Lonneke S.F. Yo³³;Jan Albert Vos⁸;Joost Bot³⁶;Pieter-Jan van Doormaal²;Anton Meijer²⁷;Elyas Ghariq¹³;Reinoud P.H. Bokkers²⁹;Marc P. van Proosdij³⁷;G. Menno Krietemeijer³³;Jo P. Peluso²⁶;Hieronymus D. Boogaarts²⁰;Rob Lo¹⁸;Wouter Dinkelaar²Auke P.A. Appelman²⁹;Bas Hammer¹⁶;Sjoert Pegge²⁷;Anouk van der Hoorn²⁹;Saman Vinke²⁰.

Writing committee

Diederik W.J. Dippel¹(chair);Aad van der Lugt²;Charles B.L.M. Majoie³;Yvo B.W.E.M. Roos⁴;Robert J. van Oostenbrugge⁵;Wim H. van Zwam⁶;Geert J. Lycklama à Nijeholt¹³;Jelis Boiten¹⁴;Jan Albert Vos⁸;Wouter J. Schonewille⁷;Jeannette Hofmeijer¹¹;Jasper M. Martens¹²;H. Bart van der Worp¹⁷;Rob H. Lo¹⁸

Adverse event committee

Robert J. van Oostenbrugge⁵(chair);Jeannette Hofmeijer¹¹;H. Zwenneke Flach²³

Trial methodologist

Hester F. Lingsma⁴⁰

Research nurses / local trial coordinators

Naziha el Ghannouti¹;Martin Sterrenberg¹;Wilma Pellikaan⁷;Rita Sprengers⁴;Marjan Elfrink¹¹;Michelle Simons¹¹;Marjolein Vossers¹²;Joke de Meris¹⁴;Tamara Vermeulen¹⁴;Annet Geerlings¹⁹;Gina van Vemde²²;Tiny Simons³⁰;Gert Messchendorp²⁸;Nynke Nicolaij²⁸;Hester Bongenaar³²;Karin Bodde²⁴;Sandra Kleijn³⁴;Jasmijn Lodico³⁴;Hanneke Droste³⁴;Maureen Wollaert⁵;Sabrina Verheesen⁵;D. Jeurissen⁵;Erna Bos⁹;Yvonne Drabbe¹⁵;Michelle Sandiman¹⁵;Nicoline Aaldering¹¹;Berber Zweedijk¹⁷;Jocova Vervoort²¹;Eva Ponjee²²;Sharon Romviel¹⁹;Karin Kanselaar¹⁹;Denn Barning¹⁰.

PhD / Medical students:

Esmee Venema⁴⁰;Vicky Chalos^{1,40};Ralph R. Geuskens³;Tim van Straaten¹⁹;Saliha Ergezen¹;Roger R.M. Harmsma¹;

Daan Muijres¹;Anouk de Jong¹;Olvert A. Berkhemer^{1,3,6};Anna M.M. Boers^{3,39};J. Huguet³;P.F.C. Groot³;Marieke A. Mens³;Katinka R. van Kranendonk³;Kilian M. Treurniet³;Manon L. Tolhuisen^{3,39};Heitor Alves³;Annick J. Weterings³;Eleonora L.F. Kirkels³;Eva J.H.F. Voogd¹¹;Lieve M. Schupp³;Sabine L. Collette^{28,29};Adrien E.D. Groot⁴;Natalie E. LeCouffe⁴;Praneeta R. Konduri³⁹;Haryadi Prasetya³⁹;Nerea Arrarte-Terrerros³⁹;Lucas A. Ramos³⁹.

List of affiliations

Department of Neurology¹, Radiology², Public Health⁴⁰, Erasmus MC University Medical Center;

Department of Radiology and Nuclear Medicine³, Neurology⁴, Biomedical Engineering & Physics³⁹, Amsterdam UMC, University of Amsterdam, Amsterdam;

Department of Neurology⁵, Radiology⁶, Maastricht University Medical Center and Cardiovascular Research Institute Maastricht (CARIM);

Department of Neurology⁷, Radiology⁸, Sint Antonius Hospital, Nieuwegein;

Department of Neurology⁹, Radiology¹⁰, Leiden University Medical Center;

Department of Neurology¹¹, Radiology¹², Rijnstate Hospital, Arnhem;

Department of Radiology¹³, Neurology¹⁴, Haaglanden MC, the Hague;

Department of Neurology¹⁵, Radiology¹⁶, HAGA Hospital, the Hague;

Department of Neurology¹⁷, Radiology¹⁸, University Medical Center Utrecht;

Department of Neurology¹⁹, Neurosurgery²⁰, Radiology²⁷, Radboud University Medical Center, Nijmegen;

Department of Neurology²¹, Radiology²⁶, Elisabeth-TweeSteden ziekenhuis, Tilburg;

Department of Neurology²², Radiology²³, Isala Klinieken, Zwolle;

Department of Neurology²⁴, Radiology²⁵, Reinier de Graaf Gasthuis, Delft;

Department of Neurology²⁸, Radiology²⁹, University Medical Center Groningen;

Department of Neurology³⁰, Radiology³¹, Atrium Medical Center, Heerlen;

Department of Neurology³², Radiology³³, Catharina Hospital, Eindhoven;

Department of Neurology³⁴, Radiology³⁵, Medisch Spectrum Twente, Enschede;

Department of Radiology³⁶, Amsterdam UMC, Vrije Universiteit van Amsterdam, Amsterdam;Department of Radiology³⁷, Noordwest Ziekenhuisgroep, Alkmaar;

Department of Radiology³⁸, Texas Stroke Institute, Texas, United States of America.

Table 4 Variables used for multiple imputation and their frequency of missing values

Variable	Frequency of missing values, n (%)
Age	0/332 (0)
Sex	0/332 (0)
Baseline NIHSS	1/332 (0)
Time from stroke onset to imaging	109/332 (33)
Intravenous alteplase	0/332 (0)
Occlusion location	14/332 (4)
Presence of hyperdense artery sign	15/332 (5)
Clot Burden Score	48/332 (15)

Table 5 Univariable and multivariable linear regression analyses for the relationship between thrombus CT characteristics and thrombus fibrin/platelet-content, in all included patients ($n = 332$)

	Unadjusted	Adjusted for clinical characteristics ^a	Adjusted for thrombus CT characteristics ^b
Hyperdense artery sign	-9.6 (-13.4 to -5.8)	-9.6 (-13.4 to -5.9)	-7.8 (-11.5 to -4.0)
Occlusion location	5.2 (3.2 to 7.1)	5.2 (3.3 to 7.2)	3.7 (0.5 to 6.8)
Clot Burden Score	1.8 (1.0 to 2.6)	1.8 (1.0 to 2.6)	0.3 (-0.9 to 1.6)

All analyses were done with fibrin/platelet content as a continuous variable, expressed as % of the thrombus. Regression coefficients are shown with 95% confidence intervals

^a Age, sex, time from stroke onset to CT and administration of IV alteplase

^b Hyperdense artery sign, occlusion location and Clot Burden Score

Table 6 Univariable and multivariable linear regression analyses for the relationship between thrombus CT characteristics and thrombus fibrin/platelet-content, in patients with available thin-slice CT imaging ($n = 94$)

	Unadjusted	Adjusted for clinical characteristics ^a	Adjusted for thrombus CT characteristics ^b
Hyperdense artery sign	-5.3 (-12.9 to 2.2)	-5.5 (-13.0 to 1.9)	3.2 (-4.5 to 10.9)
Occlusion location	4.2 (0.3 to 8.0)	3.8 (-0.1 to 7.8)	3.8 (-5.4 to 12.9)
Clot Burden Score	1.6 (0.1 to 3.1)	1.3 (-0.2 to 2.8)	-0.9 (-3.9 to 2.1)
Absolute thrombus density (HU)	-0.8 (-1.2 to -0.5)	-0.8 (-1.2 to -0.4)	-0.8 (-1.3 to -0.3)
Thrombus length (mm)	-0.8 (-1.2 to -0.4)	-0.7 (-1.2 to -0.3)	-0.7 (-1.3 to -0.1)
Relative thrombus density (HU)	-11.7 (-25.0 to 1.7)	-12.8 (-26.1 to 0.5)	10.3 (-5.7 to 26.3)
Perviousness (HU)	0.3 (0.1 to 0.6)	0.3 (0.1 to 0.6)	0.2 (-0.0 to 0.4)
DT (mm)	0.6 (0.0 to 1.1)	0.5 (-0.1 to 1.0)	-0.5 (-1.4 to 0.4)

All analyses were done with fibrin/platelet content as a continuous variable, expressed as % of the thrombus. Regression coefficients are shown with 95% confidence intervals. HU indicates Hounsfield Units and DT, distance from internal carotid artery terminus to thrombus

^a Age, sex, time from stroke onset to CT and administration of IV alteplase

^b Hyperdense artery sign, occlusion location, Clot Burden Score, absolute thrombus density, thrombus length, relative thrombus density, perviousness and distance from internal carotid artery terminus to thrombus

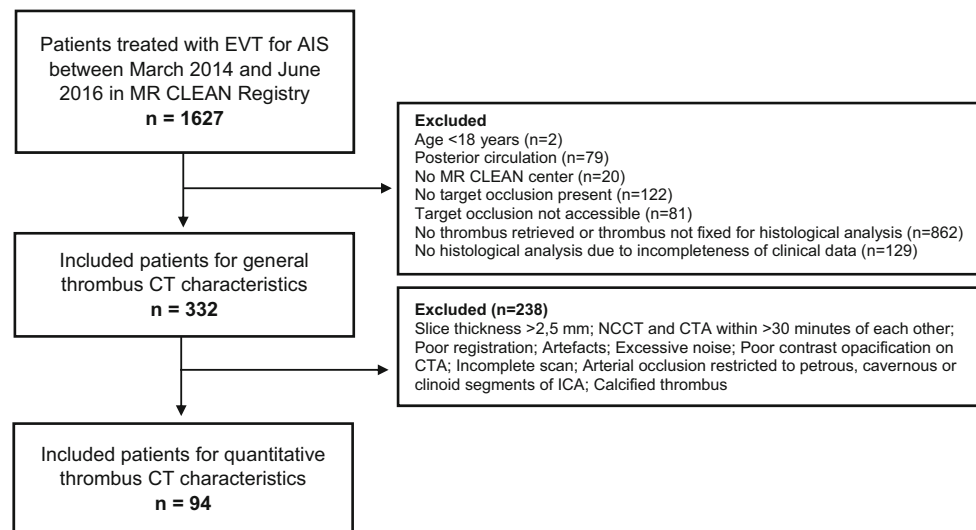


Fig. 4 Flowchart of patient inclusion. EVT indicates endovascular thrombectomy; AIS, acute ischemic stroke; NCCT, non-contrast computed tomography; CTA, computed tomography angiography and ICA, internal carotid artery

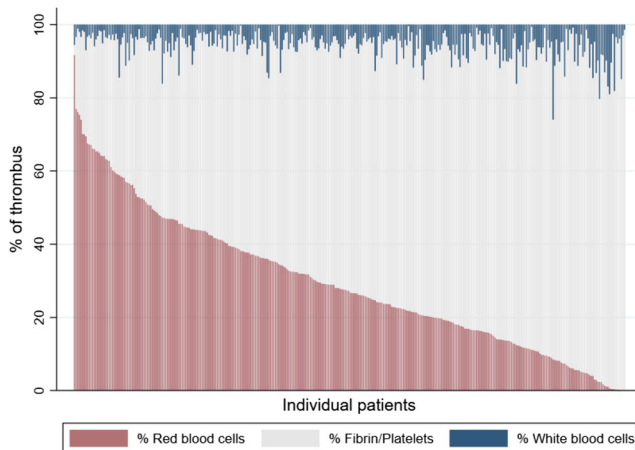


Fig. 5 Histological thrombus composition of the 332 included patients

Acknowledgements We would like to thank the MR CLEAN investigators. A list of all investigators is provided in the Appendix.

Funding This study was funded and carried out by the Erasmus University Medical Center, the Academic Medical Center Amsterdam, and the Maastricht University Medical Center. The study was additionally funded by the European Union's Horizon 2020 research and innovation program under grant agreement no. 777072 (IN-Silico trials for treatment of acute Ischemic Stroke; INSIST), which played no role in trial design and patient enrolment, nor in data collection, analysis, or writing of the manuscript.

Declarations

Ethics approval Institutional Review Board approval was obtained.

Informed consent Written informed consent was waived by the Institutional Review Board.

Conflict of interest The authors of this manuscript declare relationships with the following companies: Erasmus Medical Center received compensation from Stryker, Siemens Healthineers, and GE Healthcare for activities of A.v.d.L. Dr. Dippel and Dr. Van der Lugt report grants from Dutch Heart Foundation, grants from Brain Foundation Netherlands, grants from Health Holland Top Sector Life Sciences & Health, grants from the Netherlands Organisation for Health Research and Development, and unrestricted grants from Stryker European Operations BV; from Penumbra Inc.; from Medtronic; from Thrombolytic Science, LLC; and from Cerenovus outside the submitted work, all paid to institution. H.A.M. is co-founder and shareholder of Nicolab, a company that focuses on the use of artificial intelligence for medical image analysis. C.B.L.M. is a recipient of grants from the CVON/Dutch Heart Foundation, Stryker, European Commission, TWIN Foundation, and Health Evaluation Netherlands and is shareholder of Nicolab.

Guarantor The scientific guarantor of this publication is prof. Aad van der Lugt, Department of Radiology and Nuclear Medicine, Erasmus University Medical Center, Rotterdam, the Netherlands.

Statistics and biometry One of the authors has significant statistical expertise.

Methodology

- prospective
- observational
- multicenter study

Open Access This article is licensed under a Creative Commons Attribution 4.0 International License, which permits use, sharing, adaptation, distribution and reproduction in any medium or format, as long as you give appropriate credit to the original author(s) and the source, provide a link to the Creative Commons licence, and indicate if changes were made. The images or other third party material in this article are included in the article's Creative Commons licence, unless indicated otherwise in a credit line to the material. If material is not included in the article's Creative Commons licence and your intended use is not permitted by statutory regulation or exceeds the permitted use, you will need to obtain permission directly from the copyright holder. To view a copy of this licence, visit <http://creativecommons.org/licenses/by/4.0/>.

References

1. Yoo AJ, Andersson T (2017) Thrombectomy in acute ischemic stroke: challenges to procedural success. *J Stroke* 19(2):121–130
2. Boodt N, Snouckaert van Schauburg PRW, Hund HM et al (2021) Mechanical characterization of thrombi retrieved with endovascular thrombectomy in patients with acute ischemic stroke. *Stroke* 52(8):2510–2517
3. Maekawa K, Shibata M et al (2018) Erythrocyte-rich thrombus is associated with reduced number of maneuvers and procedure time in patients with acute ischemic stroke undergoing mechanical thrombectomy. *Cerebrovasc Dis Extra* 8(1):39–49
4. Jolugbo P, Ariens RAS (2021) Thrombus composition and efficacy of thrombolysis and thrombectomy in acute ischemic stroke. *Stroke* 52(3):1131–1142
5. Shin JW, Jeong HS, Kwon HJ, Song KS, Kim J (2018) High red blood cell composition in clots is associated with successful recanalization during intra-arterial thrombectomy. *PLoS One* 13(5):e0197492
6. Joundi RA, Menon BK (2021) Thrombus composition, imaging, and outcome prediction in acute ischemic stroke. *Neurology* 97(20 Suppl 2):S68–S78
7. Brinjikji W, Duffy S, Burrows A et al (2017) Correlation of imaging and histopathology of thrombi in acute ischemic stroke with etiology and outcome: a systematic review. *J Neurointerv Surg* 9(6):529–534
8. De Meyer SF, Andersson T, Baxter B et al (2017) Analyses of thrombi in acute ischemic stroke: a consensus statement on current knowledge and future directions. *Int J Stroke* 12(6):606–614
9. Gounis MJ, Chapot R (2017) Histological composition and the origin of the thrombus: a new diagnostic assay for secondary stroke prevention? *Stroke* 48(8):2040–2041
10. Liebeskind DS, Sanossian N, Yong WH et al (2011) CT and MRI early vessel signs reflect clot composition in acute stroke. *Stroke* 42(5):1237–1243
11. Simons N, Mitchell P, Dowling R, Gonzales M, Yan B (2015) Thrombus composition in acute ischemic stroke: a histopathological study of thrombus extracted by endovascular retrieval. *J Neuroradiol* 42(2):86–92
12. Puetz V, Dzialowski I, Hill MD et al (2008) Intracranial thrombus extent predicts clinical outcome, final infarct size and hemorrhagic transformation in ischemic stroke: the clot burden score. *Int J Stroke* 3(4):230–236
13. Santos EM, Yoo AJ, Beenen LF et al (2016) Observer variability of absolute and relative thrombus density measurements in patients with acute ischemic stroke. *Neuroradiology* 58(2):133–139
14. Santos EM, Marquering HA, den Blanken MD et al (2016) Thrombus permeability is associated with improved functional outcome and recanalization in patients with ischemic stroke. *Stroke* 47(3):732–741
15. Dutra BG, Tolhuisen ML, Alves H et al (2019) Thrombus imaging characteristics and outcomes in acute ischemic stroke patients undergoing endovascular treatment. *Stroke* 50(8):2057–2064
16. Niesten JM, van der Schaaf IC, van Dam L et al (2014) Histopathologic composition of cerebral thrombi of acute stroke patients is correlated with stroke subtype and thrombus attenuation. *PLoS One* 9(2):e88882
17. Spoms PB, Hanning U, Schwindt W et al (2017) Ischemic stroke: histological thrombus composition and pre-interventional CT attenuation are associated with intervention time and rate of secondary embolism. *Cerebrovasc Dis* 44(5-6):344–350
18. Fitzgerald S, Wang S, Dai D et al (2019) Orbit image analysis machine learning software can be used for the histological quantification of acute ischemic stroke blood clots. *PLoS One* 14(12):e0225841
19. Songsaeng D, Kaeowirun T, Sakarunchai I et al (2019) Efficacy of thrombus density on noninvasive computed tomography neuroimaging for predicting thrombus pathology and patient outcome after mechanical thrombectomy in acute ischemic stroke. *Asian J Neurosurg* 14(3):795–800
20. Boeckh-Behrens T, Schubert M, Forschler A et al (2016) The impact of histological clot composition in embolic stroke. *Clin Neuroradiol* 26(2):189–197
21. Patel TR, Fricano S, Waqas M et al (2021) Increased perviousness on CT for acute ischemic stroke is associated with fibrin/platelet-rich clots. *AJNR Am J Neuroradiol* 42(1):57–64
22. Ye G, Cao R, Lu J et al (2021) Histological composition behind CT-based thrombus density and perviousness in acute ischemic stroke. *Clin Neurol Neurosurg* 207:106804
23. Berndt M, Friedrich B, Maegerlein C et al (2018) Thrombus permeability in admission computed tomographic imaging indicates stroke pathogenesis based on thrombus histology. *Stroke* 49(11):2674–2682
24. Benson JC, Fitzgerald ST, Kadirvel R et al (2020) Clot permeability and histopathology: is a clot's perviousness on CT imaging correlated with its histologic composition? *J Neurointerv Surg* 12(1):38–42
25. Jansen IGH, Mulder M, Goldhoorn RB, investigators MCR. (2018) Endovascular treatment for acute ischaemic stroke in routine clinical practice: prospective, observational cohort study (MR CLEAN Registry). *BMJ* 360:k949
26. Staessens S, Fitzgerald S, Andersson T et al (2020) Histological stroke clot analysis after thrombectomy: technical aspects and recommendations. *Int J Stroke* 15(5):467–476
27. Klein S, Staring M, Murphy K, Viergever MA, Pluim JP (2010) elastix: a toolbox for intensity-based medical image registration. *IEEE Trans Med Imaging* 29(1):196–205
28. Riedel CH, Jensen U, Rohr A et al (2010) Assessment of thrombus in acute middle cerebral artery occlusion using thin-slice nonenhanced Computed Tomography reconstructions. *Stroke* 41(8):1659–1664
29. Friedrich B, Gawlitza M, Schob S et al (2015) Distance to thrombus in acute middle cerebral artery occlusion: a predictor of outcome after intravenous thrombolysis for acute ischemic stroke. *Stroke* 46(3):692–696
30. Duffy S, McCarthy R, Farrell M et al (2019) Per-pass analysis of thrombus composition in patients with acute ischemic stroke undergoing mechanical thrombectomy. *Stroke* 50(5):1156–1163
31. Marder VJ, Chute DJ, Starkman S et al (2006) Analysis of thrombi retrieved from cerebral arteries of patients with acute ischemic stroke. *Stroke* 37(8):2086–2093

Publisher's note Springer Nature remains neutral with regard to jurisdictional claims in published maps and institutional affiliations.

Affiliations

Hajo Hund^{1,2,3,4} · Nikki Boodt^{2,3,5}  · Nerea Arrarte Terreros^{6,7} · Aladdin Taha^{3,4} · Henk A. Marquering^{6,7} · Adriaan C. G. M. van Es^{2,8} · Reinoud P. H. Bokkers⁹ · Geert J. Lycklama à Nijeholt¹ · Charles B.L.M. Majoie⁶ · Diederik W.J. Dippel³ · Hester F. Lingsma⁵ · Heleen M. M. van Beusekom⁴ · Aad van der Lugt² · on behalf of the MR CLEAN Registry Investigators

¹ Department of Radiology, Haaglanden Medical Center, The Hague, the Netherlands

² Department of Radiology and Nuclear Medicine, Erasmus MC, University Medical Center Rotterdam, Doctor Molewaterplein 40, 3015 GD Rotterdam, the Netherlands

³ Department of Neurology, Erasmus MC, University Medical Center Rotterdam, Rotterdam, the Netherlands

⁴ Department of Cardiology, Erasmus MC, University Medical Center Rotterdam, Rotterdam, the Netherlands

⁵ Department of Public Health, Erasmus MC, University Medical Center Rotterdam, Rotterdam, the Netherlands

⁶ Department of Radiology and Nuclear Medicine, Amsterdam UMC, location AMC, Amsterdam, the Netherlands

⁷ Department of Biomedical Engineering and Physics, Amsterdam UMC, location AMC, Amsterdam, the Netherlands

⁸ Department of Radiology, Leiden University Medical Center, Leiden, the Netherlands

⁹ Department of Radiology, University Medical Center Groningen, Groningen, the Netherlands